

Flexible Quasi-Three-Dimensional Terahertz Metamaterials

Abul K. Azad,^{1,*} Hou-Tong Chen,¹ Antoinette J. Taylor,¹ Elshan

Akhadov,¹ Nina R. Weisse-Bernstein,² and John F. O'Hara¹

¹*MPA-CINT, Los Alamos National Laboratory, P. O. Box 1663,
MS K771, Los Alamos, New Mexico 87545, USA*

²*ISR-2: Space and Remote Sensing, Los Alamos National Laboratory,
P. O. Box 1663, MS B244, Los Alamos, NM 87545, USA and*

**Corresponding author: aazad@lanl.gov*

We characterize planar electric terahertz metamaterials fabricated on thin, flexible substrates using terahertz time-domain spectroscopy. Quasi-three dimensional metamaterials are formed by stacking multiple metamaterial layers. Transmission measurements reveal resonant band-stop behavior that becomes stronger with an increasing number of layers. Extracted metamaterial dielectric functions are shown to be independent of the number of layers, validating the effective medium approximation. Limitations of this approximation are discussed.

Electromagnetic metamaterials enable numerous exotic responses not available in natural materials, such as negative refractive index [1], perfect lensing [2], and cloaking [3]. They typically consist of sub-wavelength metallic resonators fabricated on dielectric or semiconducting substrates and can be made to respond to either or both of the electric and magnetic fields of incident waves. By proper scaling, individual resonators and the composite metamaterial can resonantly respond to electromagnetic waves of nearly any frequency, upto optical. Typically, the size of the resonators is roughly an order of magnitude smaller than the operating wavelength. Splitting-resonators (SRRs) in combination with wire arrays, initially introduced by Pendry, have been widely used for metamaterial designs. These structures present a considerable fabrication challenge at higher frequencies (≥ 100 GHz) and therefore microwave techniques have dominated experimental metamaterial research. This is especially relevant for bulk, or three-dimensional (3D), metamaterials, where multi-layered structures become necessary.

High frequency, multi-layer metamaterials can be fabricated by dicing and stacking single resonator arrays grown on thin substrates [4, 5]. Or they can be monolithically grown on a single substrate using multi-layer processing [6, 7]. The latter process is particularly suitable for optical metamaterials where the spacing between layers is only in the sub-micron or micron range. Either approach works for terahertz (0.1-10 THz) metamaterials though the different spacing between successive layers creates new challenges. An additional challenge, at all frequencies, is to create flexible or conformable metamaterials, which would be particularly useful in certain applications, such as cloaking or shielding. Fabrication techniques using rigid or fragile substrates, such as FR-4 or silicon, are clearly unfit. However, some progress has been made here. Multi-layer metamaterials have been demonstrated in the far-infrared frequency regime by using polyimide fillers between resonator layers [6].

In the past few years, metamaterials research has

sparked special interest in the THz community. Metamaterials are an optimistic approach to overcome the limitations of natural materials in the construction of novel functional THz devices, some of which have recently been demonstrated [8, 9, 10]. Planar SRR arrays fabricated on various semiconductor and insulator substrates have proven capable of responding to THz radiation electrically [11] and/or magnetically [12, 13]. Other designs provide an approach to negative permittivity [8] or permeability [12].

In this work, we address the issues of flexibility, 3D fabrication, and material parameter extraction by studying the transmission properties of THz metamaterials comprised of metallic electric split-ring-resonators (eSRRs) on conformable polyimide (Kapton) substrates using terahertz time domain spectroscopy (THz-TDS). These are studied as single layers and also as quasi-3D THz metamaterials by stacking up to four layers. In all cases, the measured transmission exhibits a clear minimum at 1.12 THz because of the excitation of the inductor-capacitor (LC) resonance. The transmission evolves into a full stop-band centered at the resonance frequency as the number of layers increases in the stacked quasi-bulk medium. Complex dielectric properties of the single and multiple layer samples are extracted and we show how they relate to the effective medium approximation.

The eSRR structure employed in this work is shown in Fig. 1. The square resonators of length $A = 40 \mu\text{m}$ are arranged in a square lattice of period $P = 54 \mu\text{m}$ with line width $d = 3 \mu\text{m}$, capacitor plate length $l = 12 \mu\text{m}$, and gap $g = 3 \mu\text{m}$. Using standard photolithography and e-beam evaporation, the eSRRs are fabricated in a square array on a commercially available polyimide film with a measured thickness of $84 \pm 2 \mu\text{m}$. Polyimide has been widely used for photonic and electronic devices because of its high electrical and thermal stability [14]. Its flexibility, durability, relatively low refractive index ($n \cong 2$) and absorption ($\alpha \cong 20 \text{ cm}^{-1}$) also make it favorable as a THz metamaterial substrate. Metallization consists of 10 nm of titanium followed by 200 nm of

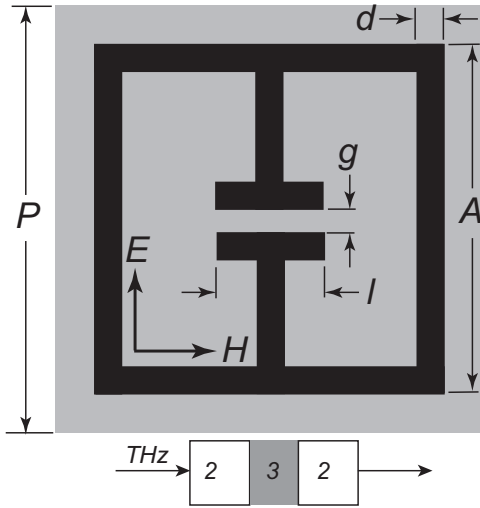


FIG. 1: Diagram of split-ring-resonator unit cell. Black area represents the metallized resonator and gray area represents the unit cell. E and H shows the orientations of incident THz electric and magnetic fields. Bottom shows the schematic of the THz propagation through the metamaterial (region 3) sandwiched between the quartz plates (region 2).

gold. During photolithography a regular silicon wafer is attached to the polyimide film to provide the mechanical support. The polyimide-based single layer metamaterials were then cut, visually aligned, and tightly stacked to form the quasi-3D media. All samples had a $10 \text{ mm} \times 10 \text{ mm}$ patterned active area.

THz transmission measurements were performed with wave incidence normal to the eSRR plane in a confocal, photoconductive antenna based THz-TDS system [15]. The system generates broadband pulsed THz radiation with a frequency independent beam waist of 3 mm diameter at the sample. Samples are placed in THz path with the gap bearing arm of the eSRR oriented parallel to the THz electric field, as shown in Fig. 1. The time-domain THz fields are recorded following passage through the samples and a dry air reference. All of the samples are sandwiched between two 1 mm thick quartz plates during measurements. Quartz has an index roughly equivalent to polyimide, which ensures that the front metamaterial layer has similar boundary conditions as subsequent layers. The reference is measured with the quartz plates in contact with each other. The complex sample $E_S(\omega)$ and reference $E_R(\omega)$ spectra are calculated by numerical Fourier transform. The effective material parameters of the sample can then be extracted from the measured transmission function $t(\omega) = E_S(\omega)/E_R(\omega)$ via [16],

$$t(\omega) = t_{23}t_{32} \frac{\exp(ik_0d(\tilde{n} - 1))}{1 + r_{23}r_{32} \exp(i2k_0d\tilde{n})}$$

where t_{23} , t_{32} and r_{23} , r_{32} are the frequency-dependent

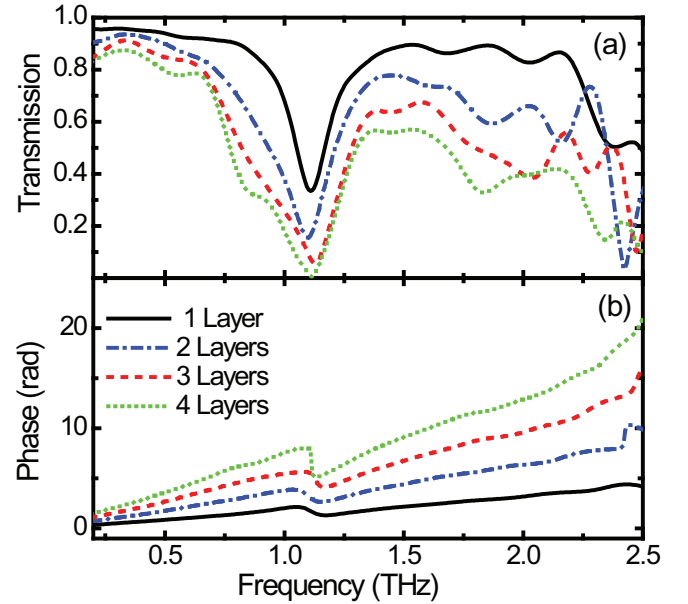


FIG. 2: (a) Measured transmission amplitude of THz electric field through metamaterial samples with different number of layers. (b) The corresponding phase change. The measurements of 1-layer, 2-layer, 3-layer, and 4-layer metamaterials are represented by solid (black), dashed-dot (blue), dashed (red), and dotted (green) curves, respectively.

complex transmission and reflection coefficients through the interfaces at the quartz-metamaterial boundaries; k_0 is the free-space wavenumber, d is the sample thickness, and $\tilde{n} = n + i\kappa$ is the sample complex refractive index. Time-windowing allows us to disregard multiple reflections in the quartz plates.

Figure 2(a) shows the measured THz amplitude following transmission through the metamaterials. Measured transmission spectra reveal clear resonances at 1.12 THz due to the effective inductive-capacitive (LC) response of the eSRRs. Transmissions were also measured through the multiple layer samples and then compared with the single layer case. The transmission spectra show band-stop behavior that increases in strength with an increasing number of layers. At four layers the effective medium becomes completely band-stop at the resonance frequency whereas the single layer transmission minimum is 33%. The low frequency off-resonance transmission also decreases from 95% in a single layer metamaterial to 85% in a four-layer metamaterial. The overall linewidth of the LC resonance increases with number of layers, though there is no significant shift in the resonance center frequency. This demonstrates that the resonance frequency is mainly determined by the SRR structural parameters. We also note the ripple features, most noticeable between the LC (1.12 THz) and dipolar (2.5 THz) resonances. Simulations initially indicate that these are due to the multiple reflections within or

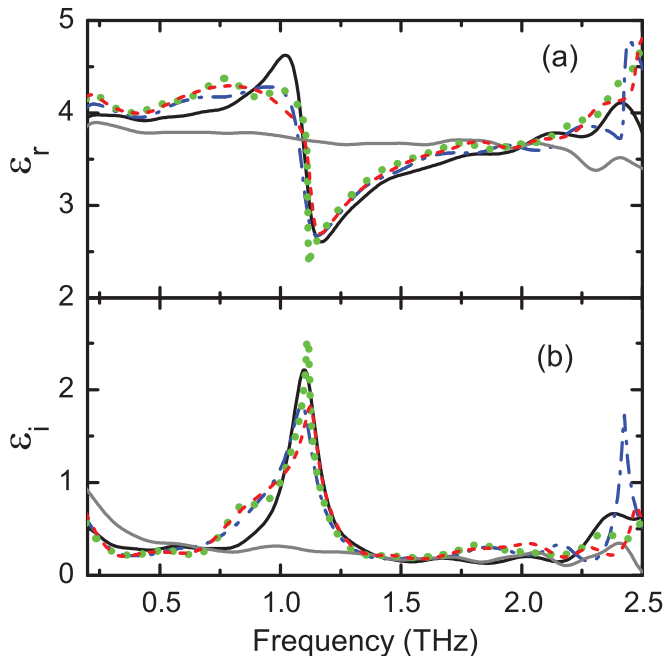


FIG. 3: Extracted (a) real and (b) imaginary dielectric functions of the effective metamaterials. They are presented using the same patterns (colors) as in Fig. 2. The solid gray curve represents the dielectric function of the bare polyimide film.

between sample layers. This is under investigation, but we presently restrict our discussion to the behavior of the LC resonance, our main interest.

Figure 2(b) shows the phase changes incurred by the THz pulses during transmission through the metamaterials. Both the substrate polyimide and the metallic eSRRs contribute to this phase change: the linear contribution comes from the substrate while the resonance structure comes from eSRRs. As expected, the slope of the linear contribution increases as the wave encounters more substrate.

The optical properties of the samples can be extracted from the measurements, but are critically dependent on the choice of some effective metamaterial thickness. Often this effective thickness is defined by enforcing a cubic unit cell for each resonator [17]. In our case this would be $54 \mu\text{m}$. Since our substrate is $84 \mu\text{m}$ thick, this approach introduces complexity in the analysis and can even cause incorrect results [16]. Instead, we simply assign each metamaterial layer the same thickness as our substrate, $84 \mu\text{m}$. The complex dielectric function is computed from the measured complex index by $\epsilon(\omega) = \epsilon_r(\omega) + i\epsilon_i(\omega) = \tilde{n}^2$. Figures 3(a) and (b) show ϵ_r and ϵ_i , respectively, for the individual and stacked metamaterials, and the bare substrate. The bare polyimide properties are fairly constant over our frequency range. The metamaterial properties are largely independent of the number of layers, in all the cases showing a

fairly flat ϵ_r averaging about 3.8 with an approximately Lorentzian perturbation of about ± 1 around resonance. The off-resonance metamaterial dielectric functions are very similar to those of the substrate with deviations that could be due to loss in the metal structures and tolerances in the substrate thickness.

Figures 2 and 3 reveal how our metamaterials behave in light of the effective media approximation. Simply expressed, $\epsilon(\omega)$ defines a material's electric response (e.g. phase shift) as a function of wave propagation distance. Thus, for homogenous media having fixed $\epsilon(\omega)$, thicker samples obviously produce larger cumulative responses. Our multi-layer samples create larger responses than the single layer (see Fig. 2), but these are distributed over greater thicknesses (more layers), yielding an unchanging $\epsilon(\omega)$. This behavior is consistent with an effective medium approximation. Though not detailed here, this approximation fails at the individual layer. For any single layer the entire resonant response is produced by the very thin SRR array [18]; it does not accumulate in passage through the substrate. For waves in transmission this fixed response is effectively distributed over the entire substrate thickness. Therefore, thicker substrates dilute the response, and ultimately flatten the Lorentzian variation in $\epsilon(\omega)$. This behavior is obviously not characteristic of a truly homogeneous medium and marks an important limitation of the effective medium treatment when applied to planar metamaterials.

In conclusion, we have demonstrated THz metamaterials based on eSRRs arrays fabricated on flexible, thin polyimide substrates and compared the transmission properties of the single-layer and quasi-3D bulk metamaterials using THz-TDS. Our results further verify a fabrication approach by which truly bulk 3D, durable, and conformable metamaterials can be realized; these are obviously important steps in realizing functional THz metamaterial devices such as prisms, lenses, waveguides, filters, and cloaks or shields. Finally, our results illustrate interesting details about the proper application of the effective medium approximation as it applies to planar metamaterials. This work was performed, in part, at the Center for Integrated Nanotechnologies, a U. S. Department of Energy, Office of Basic Energy Sciences nanoscale science research center jointly operated by Los Alamos and Sandia National Laboratories. Los Alamos National Laboratory, an affirmative action equal opportunity employer, is operated by Los Alamos National Security, LLC, for the National Nuclear Security Administration of the U. S. Department of Energy under contract DE-AC52-06NA25396. We gratefully acknowledge the support of the U.S. Department of Energy through the LANL/LDRD Program for this work.

-
- [1] R. A. Shelby, D. R. Smith, and S. Schultz, "Experimental Verification of a Negative Index of Refraction," *Science* **292**, 77-79 (2001).
- [2] J. B. Pendry, "Negative Refraction Makes a Perfect Lens," *Phys. Rev. Lett.* **85**, 3966-3969 (2000).
- [3] D. Schurig, J. J. Mock, B. J. Justice, S. A. Cummer, J. B. Pendry, A. F. Starr, and D. R. Smith, "Metamaterial Electromagnetic Cloak at Microwave Frequencies," *Science* **314**, 977-980 (2006).
- [4] M. Gokkavas, K. Guven, I. Bulu, K. Aydin, R. S. Penciu, M. Kafesaki, C. M. Soukoulis, and E. Ozbay, "Experimental demonstration of a left-handed metamaterial operating at 100 GHz," *Phys. Rev. B* **73**, 193103 (2006).
- [5] B. D. F. Casse, H. O. Moser, J. W. Lee, M. Bahou, S. Inglis, and L. K. Jian, "Towards three-dimensional and multilayer rod-split-ring metamaterial structures by means of deep x-ray lithography," *Appl. Phys. Lett.* **90**, 254106 (2007).
- [6] N. Katsarakis, G. Konstantinidis, A. Kostopoulos, R. S. Penciu, T. F. Gundogdu, M. Kafesaki, E. N. Economou, Th. Koschny, and C. M. Soukoulis, "Magnetic response of split-ring resonators in the far-infrared frequency regime," *Opt. Lett.* **30**, 1348-1350 (2005).
- [7] N. Liu, H. Guo, L. Fu, S. Kaiser, H. Schweizer, and H. Giessen, "Three-dimensional photonic metamaterials at optical frequencies," *Nature Mat.* **7**, 31-35 (2007).
- [8] H.-T. Chen, W. J. Padilla, J. M. O. Zide, A. C. Gossard, A. J. Taylor, and R. D. Averitt, "Active terahertz metamaterial devices," *Nature* **444**, 597-600 (2006).
- [9] W. J. Padilla, A. J. Taylor, C. Highstrete, M. Lee, and R. D. Averitt, "Dynamical Electric and Magnetic Metamaterial Response at Terahertz Frequencies," *Phys. Rev. Lett.*, **96**, 107401-4 (2006).
- [10] H.-T. Chen, W. J. Padilla, J. M. O. Zide, S. R. Bank, A. C. Gossard, A. J. Taylor, and R. D. Averitt, "Ultrafast optical switching of terahertz metamaterials fabricated on ErAs/GaAs nanoisland superlattices," *Opt. Lett.* **32**, 1620-1622 (2007).
- [11] A. K. Azad, J. Dai, and Weili Zhang, "Transmission properties of terahertz pulses through subwavelength double split-ring resonators," *Opt. Lett.* **31**, 634-634 (2006).
- [12] T. J. Yen, W. J. Padilla, N. Fang, D. C. Vier, D. R. Smith, J. B. Pendry, D. N. Basov, X. Zhang, "Terahertz Magnetic Response from Artificial Materials," *Science* **303**, 1494-1496 (2004).
- [13] T. Driscoll, G. O. Andreev, D. N. Basov, S. Palit, T. Ren, J. Mock, S. Y. Cho, N. M. Jokerst, and D. R. Smith, "Quantitative investigation of a terahertz artificial magnetic resonance using oblique angle spectroscopy," *Appl. Phys. Lett.* **90**, 092508-092510 (2007).
- [14] C. P. Wong, "*Polymers for Electronic and Photonic Application*," (*Academic, London, 1992*)), p. 661.
- [15] J. F. O'Hara, J. M. O. Zide, A. C. Gossard, A. J. Taylor, and R. D. Averitt, "Enhanced terahertz detection via ErAs:GaAs nanoisland superlattices," *Appl. Phys. Lett.* **88**, 251119-251121 (2006).
- [16] W. Zhang, A. K. Azad, and D. Grischkowsky, "Terahertz studies of carrier dynamics and dielectric response of n-type, freestanding epitaxial GaN," *Appl. Phys. Lett.* **82**, 2841-2843 (2003).
- [17] D. Schurig, J. J. Mock, and D. R. Smith, "Electric-field-coupled resonators for negative permittivity metamaterials," *Appl. Phys. Lett.* **88**, 041109-041111 (2006).
- [18] J. F. O'Hara, E. Smirnova, A. K. Azad, H.-T. Chen, and A. J. Taylor, "Effects of Microstructure Variation on Macroscopic Terahertz Metafilm Properties," *Active and Passive Electronic Components*, Vol. **2007**, Article ID 49691 (2007).